

Properties of the Lennard-Jones dimeric fluid in two dimensions: An integral equation study

Tomaz Urbic and Cristiano L. Dias

Citation: [The Journal of Chemical Physics](#) **140**, 094703 (2014); doi: 10.1063/1.4867289

View online: <http://dx.doi.org/10.1063/1.4867289>

View Table of Contents: <http://scitation.aip.org/content/aip/journal/jcp/140/9?ver=pdfcov>

Published by the [AIP Publishing](#)

Articles you may be interested in

[Finite-size scaling study of the vapor-liquid critical properties of confined fluids: Crossover from three dimensions to two dimensions](#)

J. Chem. Phys. **132**, 144107 (2010); 10.1063/1.3377089

[Phase behavior of attractive and repulsive ramp fluids: Integral equation and computer simulation studies](#)

J. Chem. Phys. **126**, 244510 (2007); 10.1063/1.2748043

[A self-consistent integral equation: Bridge function and thermodynamic properties for the Lennard-Jones fluid](#)

J. Chem. Phys. **119**, 2188 (2003); 10.1063/1.1583675

[Integral equation theory of Lennard-Jones fluids: A modified Verlet bridge function approach](#)

J. Chem. Phys. **116**, 8517 (2002); 10.1063/1.1467894

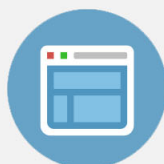
[Approximate integral equation theory for classical fluids](#)

J. Chem. Phys. **114**, 9496 (2001); 10.1063/1.1365107



Re-register for Table of Content Alerts

Create a profile.



Sign up today!



Properties of the Lennard-Jones dimeric fluid in two dimensions: An integral equation study

Tomaz Urbic^{1,a)} and Cristiano L. Dias²

¹*Faculty of Chemistry and Chemical Technology, University of Ljubljana, Aškerčeva 5, SI-1000 Ljubljana, Slovenia*

²*Physics Department, New Jersey Institute of Technology, Newark, New Jersey 07102-1982, USA*

(Received 23 January 2014; accepted 19 February 2014; published online 6 March 2014)

The thermodynamic and structural properties of the planar soft-sites dumbbell fluid are examined by Monte Carlo simulations and integral equation theory. The dimers are built of two Lennard-Jones segments. Site-site integral equation theory in two dimensions is used to calculate the site-site radial distribution functions for a range of elongations and densities and the results are compared with Monte Carlo simulations. The critical parameters for selected types of dimers were also estimated. We analyze the influence of the bond length on critical point as well as tested correctness of site-site integral equation theory with different closures. The integral equations can be used to predict the phase diagram of dimers whose molecular parameters are known. © 2014 AIP Publishing LLC. [<http://dx.doi.org/10.1063/1.4867289>]

I. INTRODUCTION

At the molecular level life is embedded in bulk water which penetrates the interior of cells through one-dimensional (1D) channels of membrane proteins. Motivated by these biological applications, several theoretical studies have been devoted to the properties of three-^{1–5} and one-dimensional⁶ fluids. In contrast, two-dimensional (2D) fluids have received much less attention. They could, however, be used to model monolayers adsorbed on solid substrates,^{7,8} or surfactant adsorbed on air/water interfaces. Accordingly, low pressure experiments of krypton adsorption on exfoliated graphite and graphitized carbon black indicated a behavior characteristic of 2D fluids.^{9,10} A 2D model was also used to study fluids confined between two parallel plates separated from each other by a few angstrom.¹¹

In addition to their interest as simple models for real situations, 1D and 2D systems have been studied to understand the effect of dimensionality on phase transitions.^{1,12–14} Reducing the dimensionality of a fluid can perturb its properties towards the solid phase. For example, it was reported that vibrational modes of water inside carbon nanotubes can exhibit properties similar to ice-like structures¹⁵ while in computer simulations water formed ice-like layers when confined between two parallel graphite sheets a few angstrom apart.¹⁶

Theoretical studies of particles interacting through various soft potentials in 2D have been addressed using different techniques.¹¹ However, the study of 2D dimers in the fluid phase is more challenging. They could be used as a model for diatomic molecules, e.g., N₂, O₂, and CO absorbed on the surface. Monolayers of dimers adsorbed on solid surfaces have been a field of intensive research.¹⁷ At a more coarse-grain level, dimers could be used to model amphiphilic molecules, e.g., methanol or lipids, when one segment of the dimer is hydrophilic and the other hydrophobic. These systems ex-

hibit interesting self-organizing properties. Most of the studies to understand dimers used computer simulations on lattice models^{18–26} and continuous-space.^{17,27,28} Here we will study 2D dimers in the fluid phase using the integral equation theory (IET) and compare theory with Monte Carlo (MC) simulations.

IET of liquids is a fast and easy-to-implement method to calculate pair distribution functions and thermodynamic properties. It provides a rather good description of fluid-phase equilibria allowing calculations to be performed along isotherms and isochores.²⁹ However, it also has drawbacks. It is based on approximations which can lead to convergence problems and even wrong results. In our study we adopt site-site integral equation theory, also known as the reference interaction site model (RISM) for molecular fluids, developed by Chandler and Andersen.³⁰ The theory is an extension of the Ornstein-Zernike (OZ) equation³¹ to a mixture of atoms, but with strong intramolecular correlations representing chemical bonds. In the original formulation,³⁰ a specific molecule was modeled as a superposition of hard spheres rigidly bonded together mimicking its atoms.³² RISM provides quite good results for the structure and thermodynamics in the dense liquid region. However, successful extension of these results to less dense liquids, as would be required to characterize the vapor-liquid coexistence curve, requires more complex treatments than first order perturbation theories considered thus far.³³ The integral equation theory based on the RISM formalism has been applied successfully to obtain structural and thermodynamic properties of various chemical, biochemical, and biological systems.^{34–38} The hard planar dumbbell fluid has been previously studied using both RISM³⁹ and molecular integral equation theory.⁴³ Comparison of RISM and MC simulations for the planar dumbbell model showed that the theory accounts qualitatively for the structure of the planar dumbbell as described by radial distribution functions but this was not the case for computed pressures.³⁹ We have to mention that methods based on RISM are not formally exact in that

^{a)}tomaz.urbic@fkkt.uni-lj.si

the graphical expansion of the RISM equations and includes incorrect terms and excludes other correct ones. The proper interaction site method (PISM)^{40,41} is a formal improvement over RISM and more accurately represents the graphical expression, but generally provides less accurate results.⁴²

Here we apply RISM to a dimeric fluid made of Lennard-Jones particles in 2D. We compute structural and thermodynamic quantities which are compared with Monte Carlo simulations. We show that under conditions of moderate density and high temperature theoretical radial distribution functions can be compared quantitatively with simulations. However, at low density, the theory reproduces only qualitatively and the simulation peaks in the radial distribution function are found at correct positions but their intensities can be either overestimated or underestimated. Also, the theory provides good estimates for the average energy of the system and the dependence of pressure with density. However, critical parameters are not reproduced accurately. This paper is organized as follows. First, we present a short description of the model, i.e., the planar soft diatomic molecules, followed by details of the Monte Carlo simulations. The theoretical framework is presented next, i.e., site-site integral equations theory with different closure relations, followed by its comparison with Monte Carlo simulations. Here we compare thermodynamic and structural properties. At the end we calculate critical behavior of the Lennard-Jones dimeric fluid by IET.

II. MODEL

In this work, a dimer is modeled as two Lennard-Jones particles at a fixed separation l . The two particles constitute sites 1 and 2 of the dimer. The potential energy for the interaction of two dimers $U(\mathbf{R}_i, \mathbf{R}_j)$ is defined as the pairwise sum of Lennard-Jones energies U_{LJ} involving constituent sites, that is,

$$U(\mathbf{R}_i, \mathbf{R}_j) = \sum_{\alpha, \beta=1}^2 U_{\text{LJ}}(|\mathbf{r}_{i\alpha} - \mathbf{r}_{j\beta}|), \quad (1)$$

where \mathbf{R}_i and \mathbf{R}_j are position vectors of centers-of-mass of dimers i and j , respectively. $\mathbf{r}_{i\alpha}$ is the position vector of site α in molecule i . A similar definition applies to $\mathbf{r}_{j\beta}$. We use the standard form of the Lennard-Jones potential,

$$U_{\text{LJ}}(r) = 4\varepsilon \left(\left(\frac{\sigma}{r} \right)^{12} - \left(\frac{\sigma}{r} \right)^6 \right), \quad (2)$$

where ε denotes the well-depth and σ is the contact parameter. In this work, we study the situation where constituent sites of the dimer are identical ($\varepsilon = \varepsilon_1 = \varepsilon_2$ and $\sigma = \sigma_1 = \sigma_2$).

III. INTEGRAL EQUATION THEORY

The site-site integral equation theory of Chandler and Andersen³⁰ provides an equation to relate the direct site-site correlation functions, $c_{\alpha\beta}(r)$, the intramolecular site-site correlation functions, $\omega_{\alpha\beta}(r)$, and the intermolecular site-site correlation functions, $h_{\alpha\beta}(r)$, between sites α and β . In Fourier space, the site-site Ornstein-Zernike-like matrix equation can

be written as

$$H(k) = \Omega(k)C(k)\Omega(k) + \rho\Omega(k)C(k)H(k), \quad (3)$$

where $H(k)$, $C(k)$, and $\Omega(k)$ are matrices whose elements are Fourier transforms of site-site correlation functions,

$$H(k) = \begin{bmatrix} h_{11}(k) & h_{12}(k) \\ h_{21}(k) & h_{22}(k) \end{bmatrix}, \quad C(k) = \begin{bmatrix} c_{11}(k) & c_{12}(k) \\ c_{21}(k) & c_{22}(k) \end{bmatrix},$$

$$\Omega(k) = \begin{bmatrix} \omega_{11}(k) & \omega_{12}(k) \\ \omega_{21}(k) & \omega_{22}(k) \end{bmatrix}. \quad (4)$$

The elements $\omega_{\alpha\beta}(k)$ are the Fourier transforms of the intramolecular correlation functions, written explicitly as³⁹

$$\omega_{\alpha\beta}(k) = J_0(kl_{\alpha\beta}), \quad (5)$$

$$\omega_{\alpha\alpha}(k) = 1, \quad (6)$$

where $l_{\alpha\beta}$ is the distance between sites α and β . $l_{\alpha\beta} = 0$ if $\beta = \alpha$ and $l_{\alpha\beta} = l$ if β is different from α and $J_0(x)$ is the Bessel function. In our case all sites are equal implying that all site-site intermolecular correlations are the same,

$$h(k) = h_{11}(k) = h_{12}(k) = h_{21}(k) = h_{22}(k) \quad (7)$$

and we can simplify our equations to OZ like equation to

$$h(k) = \frac{c(k)(1 + \omega(k))^2}{1 + 2\rho(1 + \omega(k))c(k)}, \quad (8)$$

where $\omega(k)$ is the intramolecular correlation functions between different sizes:

$$\omega(k) = \omega_{12}(k) = J_0(kl). \quad (9)$$

In order to solve the site-site OZ, we need an additional relation between $h(r)$ and $c(r)$, called the closure relation, which assumes the general form for the site-site correlation function $g(r)$ ($g(r) = h(r) + 1$),⁴⁴

$$g(r) = \exp(-\beta U(r) + h(r) - c(r) + B(r)). \quad (10)$$

β is the reverse temperature, $\beta = \frac{1}{kT}$, $U(r)$ is the site-site interaction potential, and $B(r)$ is the bridge function, which is not known. Various approximations are employed for the bridge function. The simplest option is the hypernetted chain (HNC) approximation, which neglects the bridge function ($B(r) = 0$), and simplifies the closure relation to⁴⁴

$$g(r) = \exp(-\beta U(r) + h(r) - c(r)). \quad (11)$$

Another simple approximation was proposed by Percus and Yevick^{45,46} (PY) and is written as

$$g(r) = \exp(-\beta U(r))(1 + h(r) - c(r)). \quad (12)$$

Several other closures have been developed to address the shortcomings of HNC and PY, especially a narrow region of convergence and inherent thermodynamic inconsistency. The Kovalenko-Hirata closure (KH),⁴⁷ constructed to expand the convergence region, takes the following form:

$$h(r) = \begin{cases} \exp(d(r)) - 1, & d(r) \leq 0 \\ d(r), & d(r) > 0 \end{cases},$$

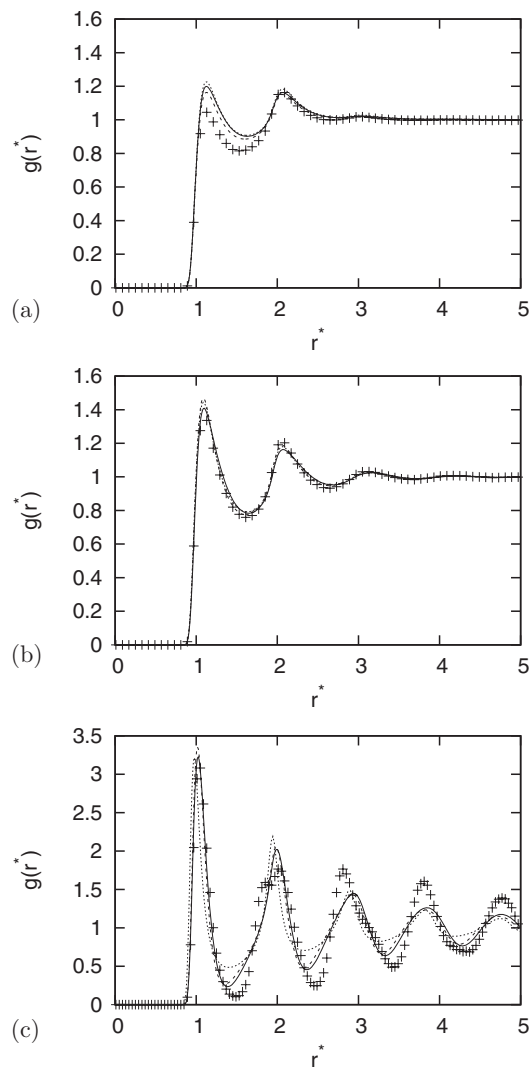


FIG. 1. Comparison of site-site correlation function for different closures with Monte Carlo simulation results for distance between sites $l^* = 1.0$ for (a) $T^* = 2.0$, $\rho^* = 0.1$, (b) $T^* = 2.0$, $\rho^* = 0.3$, and (c) $T^* = 2.0$, $\rho^* = 0.5$. Monte Carlo results are plotted with symbols, SMSA closure with solid line, PY with dashed line, and HNC with dotted line.

where $d(r) = -\beta U(r) + h(r) - c(r)$. We have also implemented the soft mean-spherical approximation (SMSA). In this closure we divide the LJ part of potential into a short-range reference part $U_0(r)$ and a longer-range perturbation part $U_1(r)$ as suggested elsewhere,⁴⁸

$$U_{LJ}(r) = U_0(r) + U_1(r), \quad (13)$$

where

$$U_0(r) = \begin{cases} U_{LJ}(r) + \varepsilon_{LJ} & r \leq r_m \\ 0 & r > r_m \end{cases}$$

and

$$U_1(r) = \begin{cases} -\varepsilon_{LJ} & r \leq r_m \\ U_{LJ}(r) & r > r_m \end{cases}.$$

The distance r_m that separates these two components is chosen to be at the position of the minimum of the LJ part of the potential function, i.e., $r_m = 2^{1/6}\sigma_{LJ}$. The SMSA closure

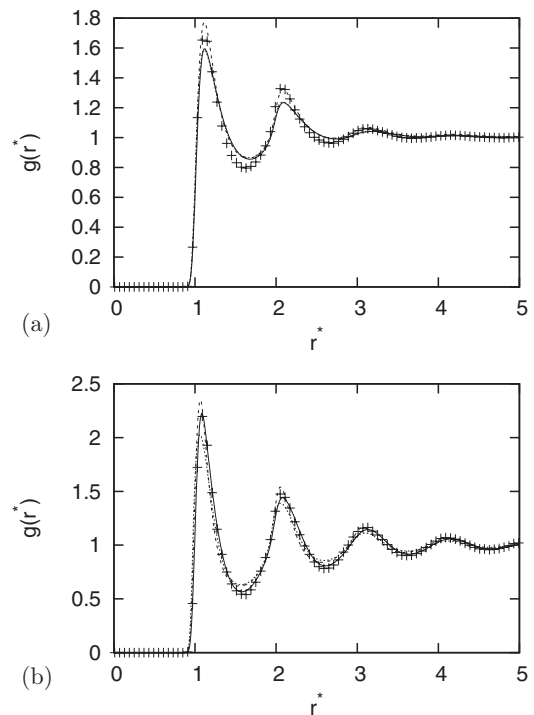


FIG. 2. Comparison of site-site correlation function for different closures with Monte Carlo simulation results for distance between sites $l^* = 1.0$ for (a) $T^* = 1.0$, $\rho^* = 0.2$ and (b) $T^* = 1.0$, $\rho^* = 0.4$. Monte Carlo results are plotted with symbols, SMSA closure with solid line, HNC with dashed line, and KH with dotted line.

relation is then written in the following form:

$$g(r) = \exp(-\beta U_0(r))(1 + h(r) - c(r) - \beta U_1(r)). \quad (14)$$

The OZ equation together with the closure condition was solved by a direct iteration. The forward and inverse Bessel-Fourier transforms, needed to couple the correlation functions in real and Fourier spaces, have been performed by the method of Talman.⁴⁹ PY is obtained as linearization of HNC closure, and SMSA and KH closures are also related to HNC closure. Since the latter is independent of dimensionality, closures derived from it are also valid in 2D. Accordingly, they have been used successfully to study several 2D problems.^{50,51} In addition to the standard closures used in the manuscript, others have been obtained to address the self-consistent problem.⁵²

Knowledge of the site-site correlation functions allows us to calculate the thermodynamic properties of interest, including the internal energy, pressure, and compressibility. The internal energy U per dimer is given by

$$U = \pi\rho \sum_{\alpha,\beta=1}^2 \int_0^\infty U_{\alpha\beta}(r)g_{\alpha\beta}(r)rdr. \quad (15)$$

The pressure can be obtained via the compressibility, virial, or energy route. Because of the approximations inherent in the theory, these three different routes do not give identical results. The compressibility of the fluid can be calculated as

$$(\rho kT\chi) = \left(\frac{\partial \rho}{\partial \beta p^c} \right) = 1 + \rho h_{\alpha\beta}(0), \quad (16)$$

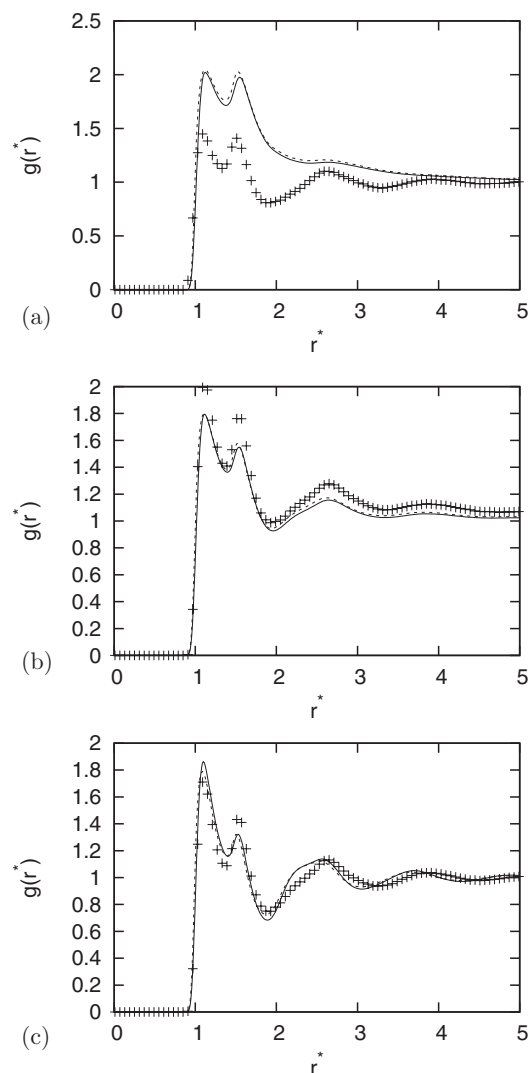


FIG. 3. Comparison of site-site correlation function for different closures with Monte Carlo simulation results for distance between sites $l^* = 0.5$ for (a) $T^* = 1.0$, $\rho^* = 0.1$, (b) $T^* = 1.0$, $\rho^* = 0.3$, and (c) $T^* = 1.0$, $\rho^* = 0.5$. Monte Carlo results are plotted with symbols, SMSA closure with solid line, and KH with dashed line.

where $h_{\alpha\beta}(0)$ is the site-site intramolecular correlation function at zero k . By integrating compressibility we calculate compressibility pressure. Virial pressure is obtained by

$$\frac{\beta p^v}{\rho} = 1 - \frac{\pi \rho \beta}{2} \sum_{\alpha, \beta=1}^2 \int_0^\infty \frac{dU_{\alpha\beta}(r)}{dr} g_{\alpha\beta}(r) r^2 dr. \quad (17)$$

Energy pressure is obtained from excess free energy per particle A by derivation at constant temperature according to

$$\frac{\beta p^e}{\rho} = \rho \left(\frac{\partial \beta A}{\partial \rho} \right)_T. \quad (18)$$

Excess free energy per particle was calculated via thermodynamic integrations along constant-density path

$$\beta A(\beta) = \beta A(\beta = 0) + \int_0^\beta U(\beta') d\beta'. \quad (19)$$

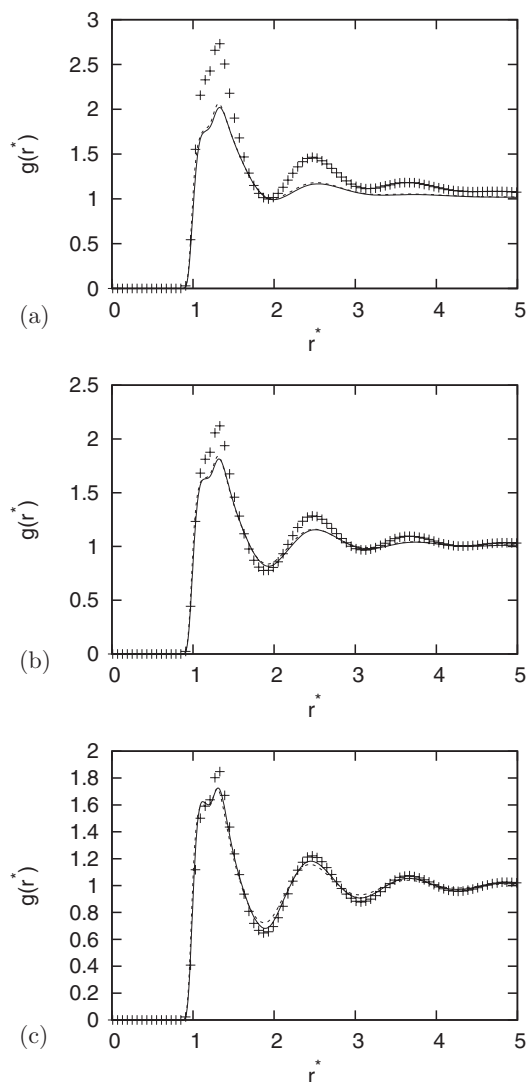


FIG. 4. Comparison of site-site correlation function for different closures with Monte Carlo simulation results for distance between sites $l^* = 0.3$ for (a) $T^* = 1.5$, $\rho^* = 0.2$, (b) $T^* = 1.5$, $\rho^* = 0.35$, and (c) $T^* = 1.5$, $\rho^* = 0.5$. Monte Carlo results are plotted with symbols, SMSA closure with solid line, and KH with dashed line.

IV. MONTE CARLO SIMULATION DETAILS

To test the theory, we perform Monte Carlo simulation of the 2D dimer model in the canonical (N,V,T) ensembles. Simulations are used to compute thermodynamic and structural properties of the model. At each step, dimers were chosen randomly and they were assigned new coordinates (x,y) and rotation. We used periodic boundary conditions and the minimum image convention to mimic an infinite system of particles. Starting configurations were selected at random. Here are some of the simulation details: 5×10^4 moves per particle were needed to equilibrate the system. Statistics were gathered over 1×10^6 moves to obtain well converged results. All simulations were performed with $N = 200$ or 400 molecules which is equivalent to about 8000 particles in 3D in case of 200 molecules in 2D. Thermodynamic quantities such as energy were calculated as statistical averages over the course of the simulations.⁵³ Pressure was calculated using the virial

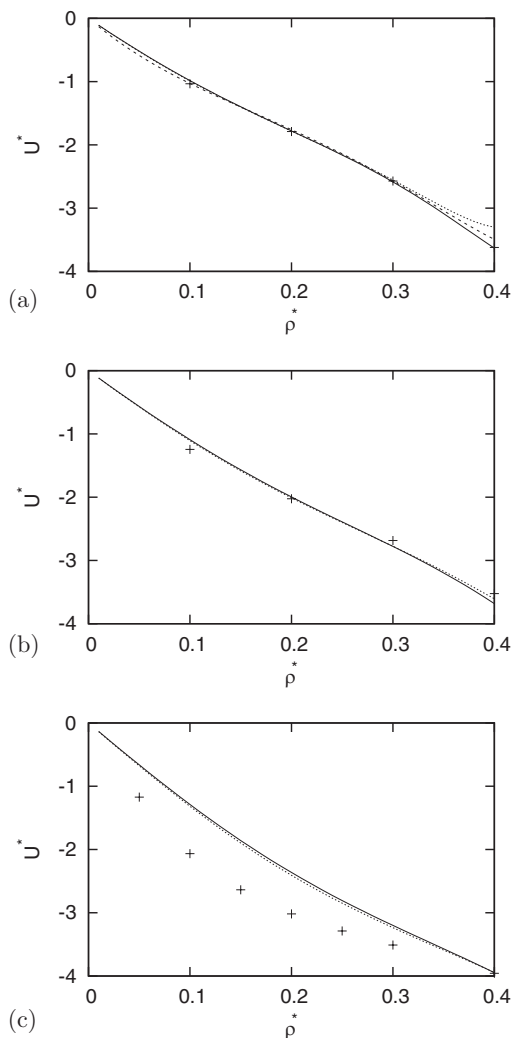


FIG. 5. Energy per dimer as a function of density for (a) $T^* = 1.0, l^* = 1.0$, (b) $T^* = 1.0, l^* = 0.75$, and (c) $T^* = 1.0, l^* = 0.5$. Monte Carlo results are plotted with symbols, SMSA closure with solid line, PY with dashed line, and KH with dotted line.

theorem. Cutoff of the potential was half-length of the simulation box.

V. RESULTS AND DISCUSSION

Results are given in reduced units: temperature and excess internal energy are normalized to the LJ interaction parameter ε ($U^* = \frac{E}{\varepsilon}, T^* = \frac{k_B T}{\varepsilon}$) and distances are scaled to the characteristic length σ ($r^* = \frac{r}{\sigma}$).

Pair distribution functions $g(r)$ were computed at various densities and temperatures using Monte Carlo simulations and site-site integral equation with four closure relations, i.e., PY, HNC, KH, and SMSA. Results from integral equations were compared with simulation results. Figures 1–4 show this comparison for different temperatures, densities, and dimer size. We used symbols for Monte Carlo results and lines for IET results.

In Fig. 1, we show the pair distribution function at different densities and high temperature. At moderate densities (Fig. 1(b)) theoretical radial distribution functions reproduce quantitatively simulation results. However, at low and high

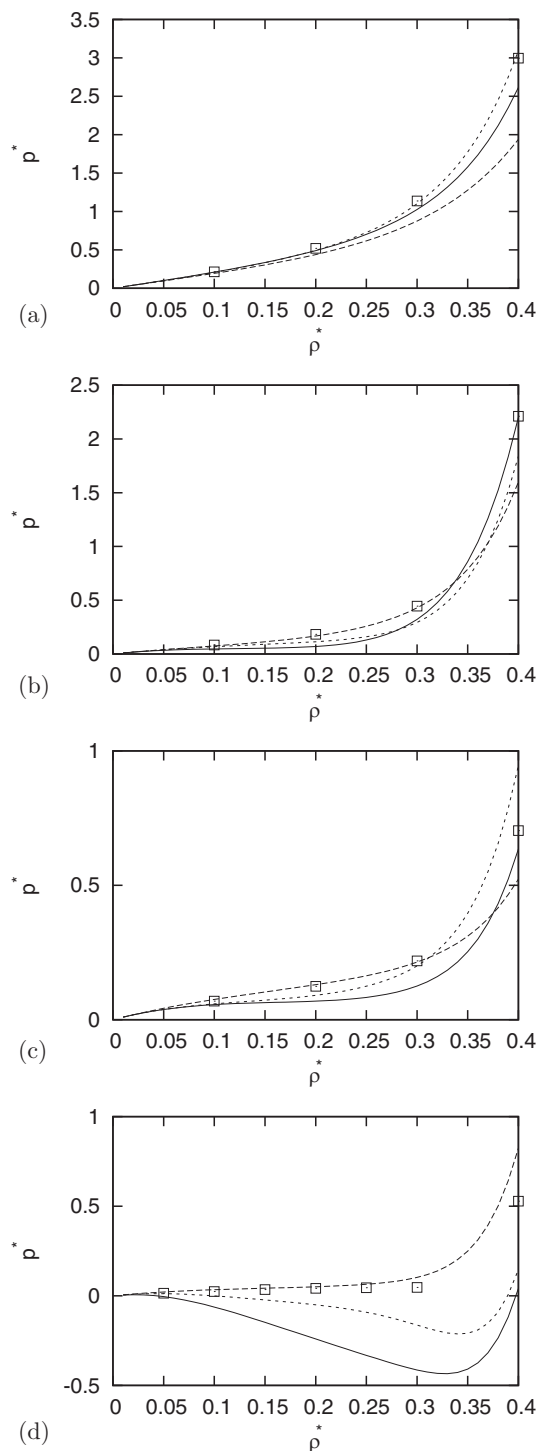


FIG. 6. Density dependence of pressure calculated by virial (solid line) compressibility (long dashed line) and energy route (dashed line) for (a) HNC and $T^* = 2.0, l^* = 0.75$, (b) PY and $T^* = 1.0, l^* = 1.0$, (c) KH and $T^* = 1.0, l^* = 0.75$, and (d) SMSA and $T^* = 0.6, l^* = 1.0$. Monte Carlo results are plotted with symbols.

densities, the theory reproduces only qualitatively the simulation: positions of main peaks in the radial distribution function are found at correct location but their intensities can be either overestimated or underestimated. Not surprisingly, for the unrealistic situations where the dimer size is smaller than the sum of van der Waals radius of its constituent sites, i.e., $l^* \ll 1$, theoretical and simulated pair distribution functions

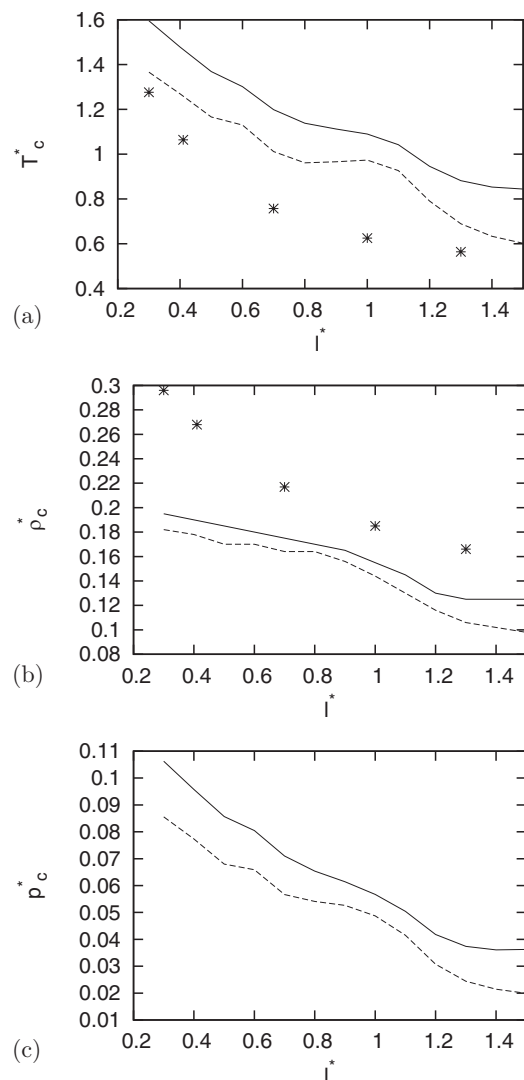


FIG. 7. (a) Critical temperature, (b) density, and (c) pressure as a function of bond distance in dimer for SMSA (solid line) and KH (dashed line) closure determined by virial pressure. Monte Carlo results by Rzyzko and Borowko¹⁷ are plotted with symbols.

show greater disagreement—see Figs. 3 and 4. Somehow the best agreement is for the SMSA and KH closures. PY and HNC closures lack the convergence when we are approaching phase transition. The incorrect behavior of the theory in the small l^* limit is associated with the appearance of unallowed graphs in the cluster expansion of the distribution functions from the site-site IET.⁵⁴

The internal energy is the difference between the translation internal energy of an ideal gas and the actual internal energy of a system. The comparison of the internal energy for computer simulation and integral equation theory are shown in Figure 5. All closures yield results that are in agreement with simulation data for distance between centers in molecule higher than $l^* > 0.7$ while for lower distance the internal energy by integral equation is too high.

SMSA, PY, HNC, and KH yield different pressures when calculated via compressibility, energy, and virial route. Figure 6 shows comparison of different pressures for selected closures and temperatures, densities, and bond distance. In

general compressibility pressure is the most accurate for all closures, but it fails to predict phase transition. Isotherm compressibility pressure for all temperatures does not show Maxwell like isotherm. Energy and virial predict liquid-gas phase transition and Figure 7 shows dependence of critical temperature, density, and pressure as a function of bond distance in dimer. Critical points were calculated by KH and SMSA closures since those were the only closures giving results at those temperatures. Virial pressure was used in determination because compressibility pressure fails in predicting phase transition and because energy pressure fails in predicting correct pressure at small bond distance. Site-site integral equation theory predicts critical point too high and critical density too low when comparing to Monte Carlo results by Rzyzko and Borowko. In integral equation results, we can see jumps in dependence at distance l^* about 0.6 and about 1.0 which are not visible in computer simulations due to limited data.

VI. CONCLUSIONS

We have examined the thermodynamics, structure, and phase transitions in 2D soft dimers, using Monte Carlo computer simulations and different variants of site-site integral equation theories with various closures: PY, HNC, SMSA, and KH. We have determined the liquid-gas critical point. The IET is somewhat less demanding from the computational point of view than the Monte Carlo simulations; however, it reproduces the structure only qualitatively. We systematically examined several closures and the results are: the PY and HNC lose convergence at low temperatures. SMSA and KH fail at predicting the proper critical point for all studied geometries of dimers. All closures also fail at structure predicting at small densities.

ACKNOWLEDGMENTS

T.U. appreciates the support of the Slovenian Research Agency (P1 0103-0201 and J1 4148) and National Institutes of Health (NIH) Grant No. GM063592. Research in C.L.D.'s lab was made possible by New Jersey Institute of Technology's startup grant.

- ¹J. A. Barker, D. Henderson, and F. F. Abraham, *Physica A* **106**, 226 (1981).
- ²J. M. Phillips, L. W. Bruch, and R. D. Murphy, *J. Chem. Phys.* **75**, 5097 (1981).
- ³O. H. Scalise, G. J. Zarragoicoechea, L. E. Gonzalez, and M. Silbert, *Mol. Phys.* **93**, 751 (1998).
- ⁴O. H. Scalise, *Phys. Chem. Liq.* **36**, 179 (1998).
- ⁵O. H. Scalise, G. J. Zarragoicoechea, and M. Silbert, *Phys. Chem. Chem. Phys.* **1**, 4241 (1999).
- ⁶A. Berezhkovskii and G. Hummer, *Phys. Rev. Lett.* **89**, 064503 (2002).
- ⁷K. S. Birdi, *Lipid and Bipolymer Monolayers at Liquid Interfaces* (Plenum Press, New York, 1989).
- ⁸S. Toxvaerd, *Mol. Phys.* **29**, 373 (1975).
- ⁹F. A. Puntam and T. Fort, *J. Phys. Chem.* **79**, 459 (1975).
- ¹⁰A. Thomy and X. Duval, *J. Chimie Physique et de Physico-Chimie Biologique* **67**, 1101 (1970).
- ¹¹T. Urbic, V. Vlasy, and K. A. Dill, *J. Phys. Chem. B* **110**, 4963 (2006).
- ¹²B. Smit and D. Frenkel, *J. Chem. Phys.* **94**, 5663 (1991).
- ¹³S. Toxvaerd, *J. Chem. Phys.* **69**, 4750 (1978).
- ¹⁴F. F. Abraham, *Phys. Rev. Lett.* **44**, 463 (1980).

- ¹⁵A. I. Kolesnikov, J.-M. Zanotti, C.-K. Loong, P. Thiyagarajan, A. P. Moravsky, R. O. Loutfy, and C. J. Burnham, *Phys. Rev. Lett.* **93**, 035503 (2004).
- ¹⁶P. Hirunsit and P. B. Balbuena, *J. Phys. Chem. C* **111**, 1709 (2007).
- ¹⁷W. Rzysko and M. Borowko, *Surf. Sci.* **605**, 1219 (2011).
- ¹⁸A. J. Phares, *J. Math. Phys.* **25**, 2169 (1984).
- ¹⁹A. J. Phares and F. J. Wunderlich, *J. Math. Phys.* **26**, 2491 (1985).
- ²⁰A. J. Ramirez-Pastor, J. L. Riccardo, and V. D. Pereyra, *Surf. Sci.* **411**, 294 (1998).
- ²¹F. Roma, J. L. Riccardo, and A. J. Ramirez-Pastor, *Phys. Rev. B* **77**, 195401 (2008).
- ²²M. Borówko and W. Rzysko, *J. Colloid Interface Sci.* **244**, 1 (2001).
- ²³W. Rzysko and M. Borowko, *J. Chem. Phys.* **117**, 4526 (2002).
- ²⁴W. Rzysko and M. Borowko, *Thin Solid Films* **425**, 304 (2003).
- ²⁵Y. Ding and J. Ni, *Phys. Rev. B* **74**, 235414 (2006).
- ²⁶N. F. Fefelov, V. A. Gorbunov, and A. V. Myshlyavtseva, *Chem. Eng. J.* **154**, 107 (2009).
- ²⁷K. W. Wojciechowski, *Phys. Rev. B* **46**, 26 (1992).
- ²⁸K. W. Wojciechowski, A. C. Branka, and D. Frenkel, *Physica A* **196**, 519 (1993).
- ²⁹M. Hus and T. Urbic, *J. Chem. Phys.* **139**, 114504 (2013).
- ³⁰D. Chandler and H. C. Andersen, *J. Chem. Phys.* **57**, 1930 (1972).
- ³¹L. S. Ornstein and F. Zernike, *Proc. Akad. Sci. (Amsterdam)* **17**, 793 (1914).
- ³²L. J. Lowden and D. Chandler, *J. Chem. Phys.* **61**, 5228 (1974).
- ³³H. C. Andersen, D. Chandler, and J. D. Weeks, *Adv. Chem. Phys.* **34**, 105 (1976).
- ³⁴M. Kinoshita, Y. Okamoto, and F. Hirata, *J. Comput. Chem.* **19**, 1724 (1998).
- ³⁵M. Kinoshita, Y. Okamoto, and F. Hirata, *J. Chem. Phys.* **110**, 4090 (1999).
- ³⁶G. N. Chuev, M. V. Fedorov, and J. Crain, *Chem. Phys. Lett.* **448**, 198 (2007).
- ³⁷G. N. Chuev and M. V. Fedorov, *J. Chem. Phys.* **131**, 074503 (2009).
- ³⁸D. Yokogawa, H. Sato, T. Imai, and S. Sakaki, *J. Chem. Phys.* **130**, 064111 (2009).
- ³⁹J. Talbot and D. J. Tildesley, *J. Chem. Phys.* **83**, 6419 (1985).
- ⁴⁰D. Chandler, R. Silbey, and B. M. Ladanyi, *Mol. Phys.* **46**, 1335 (1982).
- ⁴¹P. J. Rossky and R. A. Chiles, *Mol. Phys.* **51**, 661 (1984).
- ⁴²J. J. Howard, J. S. Perkyns, N. Choudhury, and B. M. Pettitt, *J. Chem. Theory Comput.* **4**, 1928 (2008).
- ⁴³D. A. Ward and F. Lado, *Mol. Phys.* **64**, 1185 (1988).
- ⁴⁴T. Morita and K. Hiroike, *Prog. Theor. Phys.* **23**, 829 (1960).
- ⁴⁵J. K. Percus and G. J. Yevick, *Phys. Rev.* **110**, 1 (1958).
- ⁴⁶J. K. Percus, *Phys. Rev. Lett.* **8**, 462 (1962).
- ⁴⁷A. Kovalenko and F. Hirata, *J. Chem. Phys.* **110**, 10095 (1999).
- ⁴⁸S. W. Rick and A. D. J. Haymet, *J. Chem. Phys.* **90**, 1188 (1989).
- ⁴⁹J. D. Talman, *J. Comput. Phys.* **29**, 35 (1978).
- ⁵⁰T. Urbic, *J. Chem. Phys.* **139**, 164515 (2013).
- ⁵¹T. Urbic, V. Vlachy, Yu. V. Kalyuzhnyi, N. T. Southall, and K. A. Dill, *J. Chem. Phys.* **112**, 2843 (2000).
- ⁵²G. N. Sarkisov, *Phys.-Usp.* **42**, 545 (1999).
- ⁵³D. Frenkel and B. Smit, *Molecular Simulation: From Algorithms to Applications* (Academic Press, New York, 2000).
- ⁵⁴P. A. Monson, *Mol. Phys.* **53**, 1209 (1984).